Numerical Simulations of Black Hole Spacetimes

Lee Lindblom

Theoretical Astrophysics
California Institute of Technology

Los Alamos Astrophysics Seminar
5 March 2008

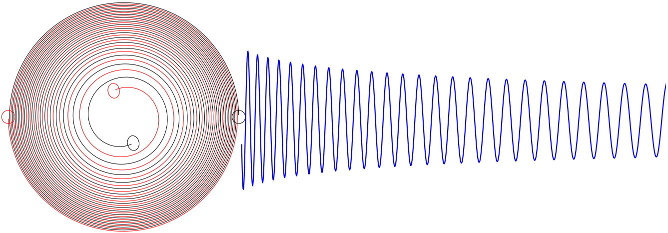

- Caltech-Cornell Numerical Relativity Collaboration

  Group leaders: Lee Lindblom, Mark Scheel, and Harald Pfeiffer at Caltech; Saul Teukolsky and Larry Kidder at Cornell.

Kidder

Lindblom

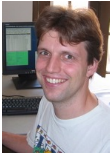

Pfeiffer

Scheel

Teukolsky

- Caltech-Cornell Numerical Relativity Collaboration

  Group leaders: Lee Lindblom, Mark Scheel, and Harald Pfeiffer at Caltech; Saul Teukolsky and Larry Kidder at Cornell.

Kidder

Lindblom

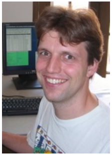

Pfeiffer

Scheel

Teukolsky

- Caltech group: Michael Boyle, Jeandrew Brink, Luisa Buchman, Tony Chu, Michael Cohen, Lee Lindblom, Keith Matthews, Harald Pfeiffer, Mark Scheel, Bela Szilagyi, Kip Thorne.
- Cornell group: Matthew Duez, Francois Foucart, Lawrence Kidder, Francois Limousin, Geoffrey Lovelace, Abdul Mroue, Robert Owen, Nick Taylor, Saul Teukolsky.

Motivation: Gravitational Wave Astronomy

- Recent work in numerical relativity is aimed at providing model waveforms for gravitational wave (GW) astronomy (LIGO, etc.).

Motivation: Gravitational Wave Astronomy

- Recent work in numerical relativity is aimed at providing model waveforms for gravitational wave (GW) astronomy (LIGO, etc.).
- Binary black hole systems emit large amounts of GW as the holes inspiral and ultimately merge. These are expected to be among the strongest sources detectable by LIGO.

Motivation: Gravitational Wave Astronomy

- Recent work in numerical relativity is aimed at providing model waveforms for gravitational wave (GW) astronomy (LIGO, etc.).
- Binary black hole systems emit large amounts of GW as the holes inspiral and ultimately merge. These are expected to be among the strongest sources detectable by LIGO.
- Numerical waveforms may be useful in detection (to construct better data filters), and/or in modeling detected signals.

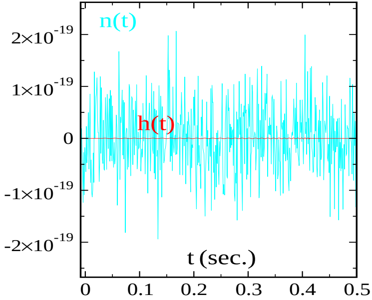

Motivation: Gravitational Wave Astronomy

- Recent work in numerical relativity is aimed at providing model waveforms for gravitational wave (GW) astronomy (LIGO, etc.).
- Binary black hole systems emit large amounts of GW as the holes inspiral and ultimately merge. These are expected to be among the strongest sources detectable by LIGO.
- Numerical waveforms may be useful in detection (to construct better data filters), and/or in modeling detected signals.

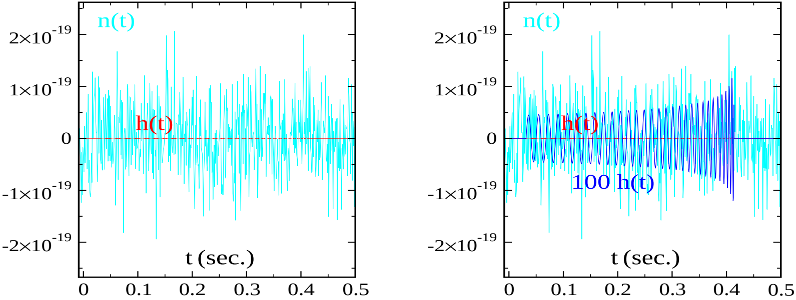

Gravitational Wave Data Analysis

- Signals $s(t)$ are detected in the noisy LIGO data by projecting them onto a template $h(\lambda, t)$ using a noise-weighted inner product:

$$\rho(\lambda) = 2\int_0^\infty \frac{\tilde{s}(f)\tilde{h}^*(f,\lambda)}{S_h(f)}df \left[\int_0^\infty \frac{\tilde{h}(f,\lambda)\tilde{h}^*(f,\lambda)}{S_h(f)}df\right]^{-1/2}.$$

Gravitational Wave Data Analysis

- Signals $s(t)$ are detected in the noisy LIGO data by projecting them onto a template $h(\lambda, t)$ using a noise-weighted inner product:

$$\rho(\lambda) = 2\int_0^\infty \frac{\tilde{s}(f)\tilde{h}^*(f,\lambda)}{S_h(f)}df\left[\int_0^\infty \frac{\tilde{h}(f,\lambda)\tilde{h}^*(f,\lambda)}{S_h(f)}df\right]^{-1/2}.$$

- The signal to noise ratio, $\rho(\lambda)$, is maximized by adjusting the template parameters λ.

Gravitational Wave Data Analysis

- Signals $s(t)$ are detected in the noisy LIGO data by projecting them onto a template $h(\lambda, t)$ using a noise-weighted inner product:

$$\rho(\lambda) = 2\int_0^\infty \frac{\tilde{s}(f)\tilde{h}^*(f,\lambda)}{S_h(f)}df \left[\int_0^\infty \frac{\tilde{h}(f,\lambda)\tilde{h}^*(f,\lambda)}{S_h(f)}df\right]^{-1/2}.$$

- The signal to noise ratio, $\rho(\lambda)$, is maximized by adjusting the template parameters λ.
- A detection occurs whenever a signal is present that matches a signal template with $\rho(\lambda) > \rho_{\min}$.

Gravitational Wave Data Analysis

- Signals $s(t)$ are detected in the noisy LIGO data by projecting them onto a template $h(\lambda, t)$ using a noise-weighted inner product:

$$\rho(\lambda) = 2\int_0^\infty \frac{\tilde{s}(f)\tilde{h}^*(f,\lambda)}{S_h(f)}df \left[\int_0^\infty \frac{\tilde{h}(f,\lambda)\tilde{h}^*(f,\lambda)}{S_h(f)}df\right]^{-1/2}.$$

- The signal to noise ratio, $\rho(\lambda)$, is maximized by adjusting the template parameters λ.
- A detection occurs whenever a signal is present that matches a signal template with $\rho(\lambda) > \rho_{\text{min}}$. For LIGO searches $\rho_{\text{min}} \approx 8$.

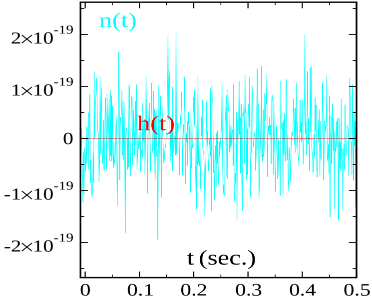

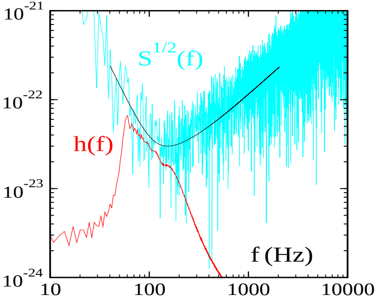

Why Is Numerical Relativity So Difficult?

- Dynamics of binary black hole problem is driven by delicate adjustments to orbit due to emission of gravitational waves.
- Very big computational problem:
  - Must evolve ~ 50 dynamical fields (spacetime metric plus all first derivatives).
  - Must accurately resolve features on many scales from black hole horizons $r \sim GM/c^2$ to emitted waves $r \sim 100GM/c^2$.
  - Many grid points are required $\gtrsim 10^6$ even if points are located optimally.

Why Is Numerical Relativity So Difficult?

- Dynamics of binary black hole problem is driven by delicate adjustments to orbit due to emission of gravitational waves.
- Very big computational problem:
  - Must evolve ~ 50 dynamical fields (spacetime metric plus all first derivatives).
  - Must accurately resolve features on many scales from black hole horizons $r \sim GM/c^2$ to emitted waves $r \sim 100GM/c^2$.
  - Many grid points are required $\gtrsim 10^6$ even if points are located optimally.
- Most representations of the Einstein equations have mathematically ill-posed initial value problems.
- Constraint violating instabilities destroy stable numerical solutions in many well-posed forms of the equations.

Unstable BBH Movie

Recent Progress in Numerical Relativity

- Frans Pretorius performs first numerical BBH inspiral, merger and ringdown calculations in the spring of 2005 using a “generalized harmonic” formulation of the Einstein equations. Pretorius Inspiral Movie

Recent Progress in Numerical Relativity

- Frans Pretorius performs first numerical BBH inspiral, merger and ringdown calculations in the spring of 2005 using a "generalized harmonic" formulation of the Einstein equations. Pretorius Inspiral Movie
- Groups at NASA GSFC and U. Texas–Brownsville simultaneously announce similar BBH simulations in the fall of 2005 using very different methods (BSSN–puncture).
  LSU/AEI collaboration obtains similar results in Dec. 2005.
- Penn State group begins the study of physical properties of BBH orbits in early 2006 by evolving unequal mass binaries and measuring the kick velocity using BSSN–puncture methods.
- ...

Outline of Remainder of Talk:

- Technical issues:
  - Constraint Damping.
  - Pseudo-Spectral Methods.
  - Feedback Control Systems.
- Science results:
  - Compare numerical waveforms with post-Newtonian approximations.

Gauge and Constraints in Electromagnetism

- The usual representation of the vacuum Maxwell equations split into evolution equations and constraints:

$$\partial_t \vec{E} = \vec{\nabla} \times \vec{B}, \qquad \nabla \cdot \vec{E} = 0,$$
$$\partial_t \vec{B} = -\vec{\nabla} \times \vec{E}, \qquad \nabla \cdot \vec{B} = 0.$$

  These equations are often written in the more compact 4-dimensional notation: $\nabla^a F_{ab} = 0$ and $\nabla_{[a} F_{bc]} = 0$, where F_{ab} has components $\vec{E}$ and $\vec{B}$.

Gauge and Constraints in Electromagnetism

- The usual representation of the vacuum Maxwell equations split into evolution equations and constraints:

$$\partial_t \vec{E} = \vec{\nabla} \times \vec{B}, \qquad \nabla \cdot \vec{E} = 0,$$
$$\partial_t \vec{B} = -\vec{\nabla} \times \vec{E}, \qquad \nabla \cdot \vec{B} = 0.$$

  These equations are often written in the more compact 4-dimensional notation: $\nabla^a F_{ab} = 0$ and $\nabla_{[a} F_{bc]} = 0$, where F_{ab} has components $\vec{E}$ and $\vec{B}$.

- Maxwell's equations are often re-expressed in terms of a vector potential $F_{ab} = \nabla_a A_b - \nabla_b A_a$:

$$\nabla^a \nabla_a A_b - \nabla_b \nabla^a A_a = 0.$$

Gauge and Constraints in Electromagnetism

- The usual representation of the vacuum Maxwell equations split into evolution equations and constraints:
$$\partial_t \vec{E} = \vec{\nabla} \times \vec{B}, \qquad \nabla \cdot \vec{E} = 0,$$
$$\partial_t \vec{B} = -\vec{\nabla} \times \vec{E}, \qquad \nabla \cdot \vec{B} = 0.$$
These equations are often written in the more compact 4-dimensional notation: $\nabla^a F_{ab} = 0$ and $\nabla_{[a} F_{bc]} = 0$, where F_{ab} has components $\vec{E}$ and $\vec{B}$.
- Maxwell's equations are often re-expressed in terms of a vector potential $F_{ab} = \nabla_a A_b - \nabla_b A_a$:
$$\nabla^a \nabla_a A_b - \nabla_b \nabla^a A_a = 0.$$
- This form of Maxwell's equations is manifestly hyperbolic as long as the gauge is chosen correctly, e.g., let $\nabla^a A_a = H(x,t)$, giving:
$$\nabla^a \nabla_a A_b \equiv \left(-\partial_t^2 + \partial_x^2 + \partial_y^2 + \partial_z^2\right) A_b = \nabla_b H.$$

Constraint Damping

- Where are the constraints: $\nabla^a\nabla_a A_b = \nabla_b H$?

Constraint Damping

- Where are the constraints: $\nabla^a\nabla_a A_b = \nabla_b H$?
- Gauge condition becomes a constraint: $0 = \mathcal{C} \equiv \nabla^a A_a - H$.
- Maxwell's equations imply that this constraint is preserved:

$$\nabla^a\nabla_a \mathcal{C} = 0.$$

Constraint Damping

- Where are the constraints: $\nabla^a\nabla_a A_b = \nabla_b H$?
- Gauge condition becomes a constraint: $0 = \mathcal{C} \equiv \nabla^a A_a - H$.
- Maxwell's equations imply that this constraint is preserved:

$$\nabla^a\nabla_a \mathcal{C} = 0.$$

- Modify evolution equations by adding multiples of the constraints:

$$\nabla^a\nabla_a A_b = \nabla_b H + \gamma_0 t_b \mathcal{C} = \nabla_b H + \gamma_0 t_b (\nabla^a A_a - H).$$

- These changes also affect the constraint evolution equation,

$$\nabla^a\nabla_a \mathcal{C} - \gamma_0 t^b \nabla_b \mathcal{C} = 0,$$

so constraint violations are damped when $\gamma_0 > 0$.

Constraint Damped Einstein System

- "Generalized Harmonic" form of Einstein's equations have properties similar to Maxwell's equations:
  - Gauge (coordinate) conditions are imposed by specifying the divergence of the spacetime metric: $\partial_a g^{ab} = H^b + \ldots$
  - Evolution equations become manifestly hyperbolic: $\Box g_{ab} = \ldots$
  - Gauge conditions become constraints.
  - Constraint damping terms can be added which make numerical evolutions stable.

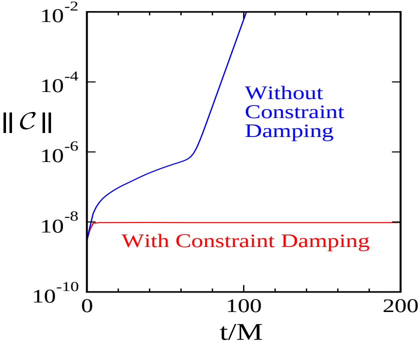

Numerical Solution of Evolution Equations

$$\partial_t u = F(u, \partial_x u, x, t).$$

- Choose a grid of spatial points, x_n.

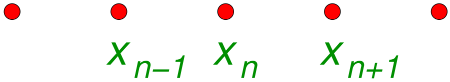

Numerical Solution of Evolution Equations

$$\partial_t u = F(u, \partial_x u, x, t).$$

- Choose a grid of spatial points, x_n.
- Evaluate the function u on this grid: $u_n(t) = u(x_n, t)$.

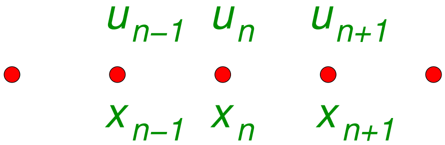

Numerical Solution of Evolution Equations

$$\partial_t u = F(u, \partial_x u, x, t).$$

- Choose a grid of spatial points, x_n.
- Evaluate the function u on this grid: $u_n(t) = u(x_n, t)$.

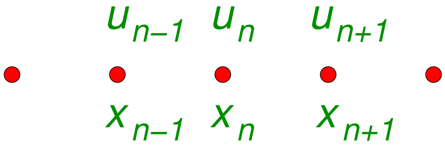

- Approximate the spatial derivatives at the grid points
  $\partial_x u(x_n) = \sum_k D_{n\,k} u_k$.

Numerical Solution of Evolution Equations

$$\partial_t u = F(u, \partial_x u, x, t).$$

- Choose a grid of spatial points, x_n.
- Evaluate the function u on this grid: $u_n(t) = u(x_n, t)$.

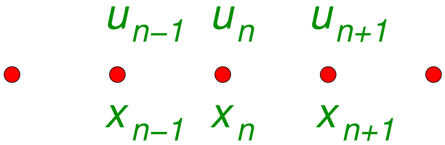

- Approximate the spatial derivatives at the grid points
$\partial_x u(x_n) = \sum_k D_{nk} u_k$.
- Evaluate F at the grid points x_n in terms of the u_k: $F(u_k, x_n, t)$.

Numerical Solution of Evolution Equations

$$\partial_t u = F(u, \partial_x u, x, t).$$

- Choose a grid of spatial points, x_n.
- Evaluate the function u on this grid: $u_n(t) = u(x_n, t)$.

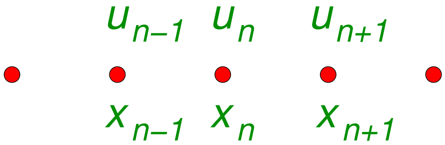

- Approximate the spatial derivatives at the grid points
  $\partial_x u(x_n) = \sum_k D_{n\,k} u_k$.
- Evaluate F at the grid points x_n in terms of the u_k: $F(u_k, x_n, t)$.
- Solve the coupled system of ordinary differential equations,

$$\frac{du_n(t)}{dt} = F[u_k(t), x_n, t],$$

using standard numerical methods (e.g. Runge-Kutta).

Basic Numerical Methods

- Different numerical methods use different ways of choosing the grid points x_n, and different expressions for the spatial derivatives $\partial_x u(u_n) = \sum_k D_{n\,k} u_k$.

Basic Numerical Methods

- Different numerical methods use different ways of choosing the grid points x_n, and different expressions for the spatial derivatives $\partial_x u(u_n) = \sum_k D_{n\,k} u_k$.

- Most numerical groups use finite difference methods:
  - Uniformly spaced grids: $x_n - x_{n-1} = \Delta x =$ constant.
  - Use Taylor expansions,

$$u_{n-1} = u(x_n - \Delta x) = u(x_n) - \partial_x u(x_n)\Delta x + \partial_x^2 u(x_n)\Delta x^2/2 + \mathcal{O}(\Delta x^3),$$
$$u_{n+1} = u(x_n + \Delta x) = u(x_n) + \partial_x u(x_n)\Delta x + \partial_x^2 u(x_n)\Delta x^2/2 + \mathcal{O}(\Delta x^3),$$

to obtain the needed expressions for $\partial_x u$:

$$\partial_x u(x_n) = \frac{u_{n+1} - u_{n-1}}{2\Delta x} + \mathcal{O}(\Delta x^2).$$

Basic Numerical Methods

- Different numerical methods use different ways of choosing the grid points x_n, and different expressions for the spatial derivatives $\partial_x u(u_n) = \sum_k D_{n\,k} u_k$.
- Most numerical groups use finite difference methods:
  - Uniformly spaced grids: $x_n - x_{n-1} = \Delta x =$ constant.
  - Use Taylor expansions,

$$u_{n-1} = u(x_n - \Delta x) = u(x_n) - \partial_x u(x_n)\Delta x + \partial_x^2 u(x_n)\Delta x^2/2 + \mathcal{O}(\Delta x^3),$$
$$u_{n+1} = u(x_n + \Delta x) = u(x_n) + \partial_x u(x_n)\Delta x + \partial_x^2 u(x_n)\Delta x^2/2 + \mathcal{O}(\Delta x^3),$$

  to obtain the needed expressions for $\partial_x u$:

$$\partial_x u(x_n) = \frac{u_{n+1} - u_{n-1}}{2\Delta x} + \mathcal{O}(\Delta x^2).$$

- Grid spacing decreases as the number of grid points N increases, $\Delta x \sim 1/N$. Errors in finite difference methods scale as N^{-p}.

Basic Numerical Methods II

- A few groups (including ours) use pseudo-spectral methods.

Basic Numerical Methods II

- A few groups (including ours) use pseudo-spectral methods.
- Represent functions as finite sums: $u(x,t) = \sum_{k=0}^{N-1} \tilde{u}_k(t) e^{ikx}$.
- Choose grid points x_n to allow exact (and efficient) inversion of the series: $\tilde{u}_k(t) = \sum_{n=0}^{N-1} w_n \, u(x_n, t) e^{-ikx_n}$.

Basic Numerical Methods II

- A few groups (including ours) use pseudo-spectral methods.
- Represent functions as finite sums: $u(x,t) = \sum_{k=0}^{N-1} \tilde{u}_k(t) e^{ikx}$.
- Choose grid points x_n to allow exact (and efficient) inversion of the series: $\tilde{u}_k(t) = \sum_{n=0}^{N-1} w_n\, u(x_n,t) e^{-ikx_n}$.
- Obtain derivative formulas by differentiating the series: $\partial_x u(x_n,t) = \sum_{k=0}^{N-1} \tilde{u}_k(t) \partial_x e^{ikx_n} = \sum_{m=0}^{N-1} D_{n\,m}\, u(x_m,t)$.

Basic Numerical Methods II

- A few groups (including ours) use pseudo-spectral methods.
- Represent functions as finite sums: $u(x,t) = \sum_{k=0}^{N-1} \tilde{u}_k(t) e^{ikx}$.
- Choose grid points x_n to allow exact (and efficient) inversion of the series: $\tilde{u}_k(t) = \sum_{n=0}^{N-1} w_n\, u(x_n,t) e^{-ikx_n}$.
- Obtain derivative formulas by differentiating the series: $\partial_x u(x_n,t) = \sum_{k=0}^{N-1} \tilde{u}_k(t) \partial_x e^{ikx_n} = \sum_{m=0}^{N-1} D_{n\,m}\, u(x_m,t)$.
- Errors in spectral methods are dominated by the size of $\tilde{u}_N$.
- Estimate the errors (for Fourier series of *smooth* functions):

$$\begin{aligned}\tilde{u}_N &= \frac{1}{2\pi}\int_{-\pi}^{\pi} u(x) e^{-iNx} dx = \frac{1}{2\pi}\left(\frac{-i}{N}\right)\int_{-\pi}^{\pi}\frac{du(x)}{dx} e^{-iNx} dx \\ &= \frac{1}{2\pi}\left(\frac{-i}{N}\right)^p \int_{-\pi}^{\pi}\frac{d^p u(x)}{dx^p} e^{-iNx} dx \leq \frac{1}{N^p}\max\left|\frac{d^p u(x)}{dx^p}\right|.\end{aligned}$$

Basic Numerical Methods II

- A few groups (including ours) use pseudo-spectral methods.
- Represent functions as finite sums: $u(x,t) = \sum_{k=0}^{N-1} \tilde{u}_k(t) e^{ikx}$.
- Choose grid points x_n to allow exact (and efficient) inversion of the series: $\tilde{u}_k(t) = \sum_{n=0}^{N-1} w_n\, u(x_n, t) e^{-ikx_n}$.
- Obtain derivative formulas by differentiating the series: $\partial_x u(x_n, t) = \sum_{k=0}^{N-1} \tilde{u}_k(t) \partial_x e^{ikx_n} = \sum_{m=0}^{N-1} D_{n\,m}\, u(x_m, t)$.
- Errors in spectral methods are dominated by the size of $\tilde{u}_N$.
- Estimate the errors (for Fourier series of *smooth* functions):

$$\begin{aligned} \tilde{u}_N &= \frac{1}{2\pi}\int_{-\pi}^{\pi} u(x) e^{-iNx} dx = \frac{1}{2\pi}\left(\frac{-i}{N}\right)\int_{-\pi}^{\pi} \frac{du(x)}{dx} e^{-iNx} dx \\ &= \frac{1}{2\pi}\left(\frac{-i}{N}\right)^p \int_{-\pi}^{\pi} \frac{d^p u(x)}{dx^p} e^{-iNx} dx \leq \frac{1}{N^p} \max\left|\frac{d^p u(x)}{dx^p}\right|. \end{aligned}$$

- Errors in spectral methods decrease faster than any power of N.

Comparing Different Numerical Methods

- Wave propagation with second-order finite difference method:

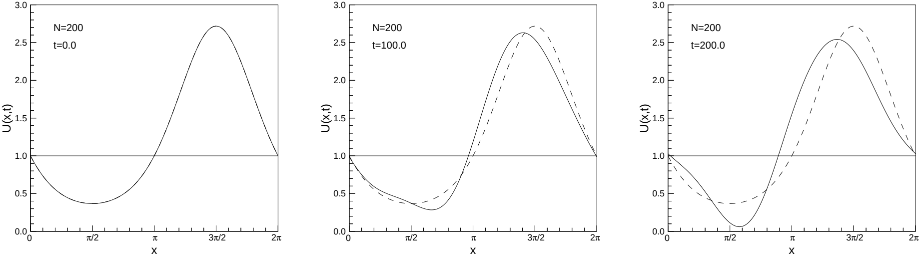

Figures from Hesthaven, Gottlieb, & Gottlieb (2007).

Comparing Different Numerical Methods

- Wave propagation with second-order finite difference method:

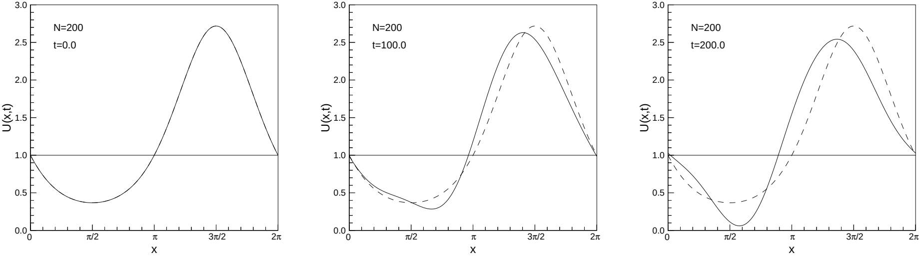

- Wave propagation with spectral method:

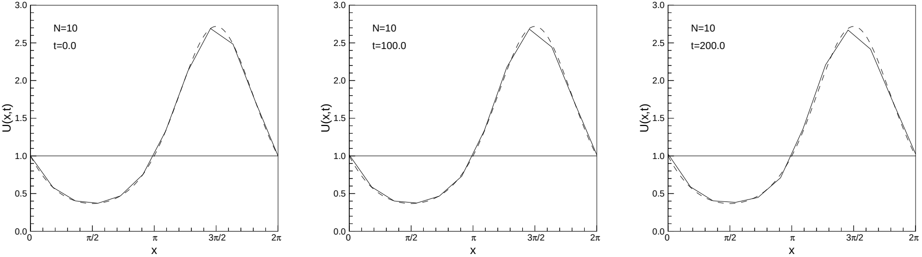

Figures from Hesthaven, Gottlieb, & Gottlieb (2007).

Moving Black Holes

- Black hole interior is not in causal contact with exterior. Interior is removed, introducing an excision boundary.

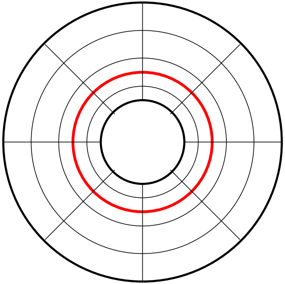

Moving Black Holes

- Black hole interior is not in causal contact with exterior. Interior is removed, introducing an excision boundary.
- Numerical grid must be moved when black holes move too far.

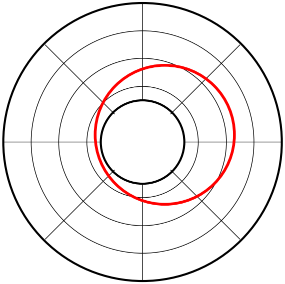

Moving Black Holes

- Black hole interior is not in causal contact with exterior. Interior is removed, introducing an excision boundary.
- Numerical grid must be moved when black holes move too far.

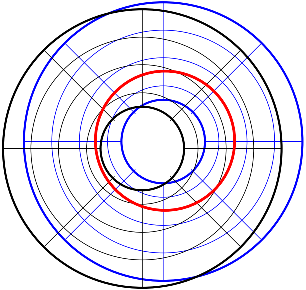

Moving Black Holes

- Black hole interior is not in causal contact with exterior.
  Interior is removed, introducing an excision boundary.
- Numerical grid must be moved when black holes move too far.

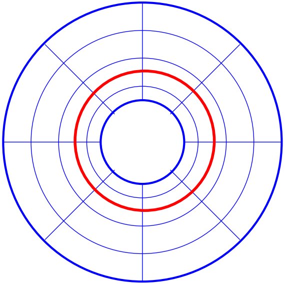

Moving Black Holes

- Black hole interior is not in causal contact with exterior. Interior is removed, introducing an excision boundary.
- Numerical grid must be moved when black holes move too far.
- Problems:
  - Difficult to get smooth extrapolation at trailing edge of horizon.

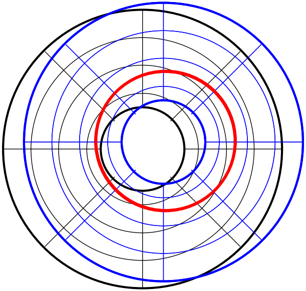

Moving Black Holes

- Black hole interior is not in causal contact with exterior. Interior is removed, introducing an excision boundary.
- Numerical grid must be moved when black holes move too far.
- Problems:
  - Difficult to get smooth extrapolation at trailing edge of horizon.
  - Causality trouble at leading edge of horizon.

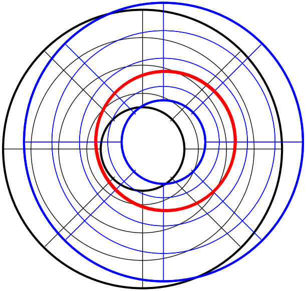

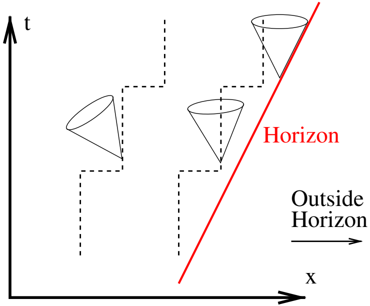

Moving Black Holes

- Black hole interior is not in causal contact with exterior. Interior is removed, introducing an excision boundary.
- Numerical grid must be moved when black holes move too far.
- Problems:
  - Difficult to get smooth extrapolation at trailing edge of horizon.
  - Causality trouble at leading edge of horizon.
- Solution:
  Choose coordinates that smoothly track the motions of the centers of the black holes.

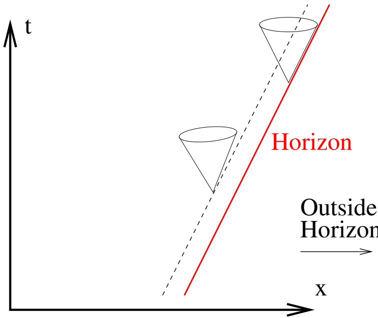

Horizon Tracking Coordinates

- Coordinates must be used that track the motions of the holes.
- A coordinate transformation from "inertial" coordinates, $(\bar{x}, \bar{y}, \bar{z})$, to "co-moving" coordinates (x, y, z), consisting of a rotation followed by an expansion,

$$\begin{pmatrix} x \\ y \\ z \end{pmatrix} = e^{a(\bar{t})} \begin{pmatrix} \cos\varphi(\bar{t}) & -\sin\varphi(\bar{t}) & 0 \\ \sin\varphi(\bar{t}) & \cos\varphi(\bar{t}) & 0 \\ 0 & 0 & 1 \end{pmatrix} \begin{pmatrix} \bar{x} \\ \bar{y} \\ \bar{z} \end{pmatrix},$$

  is general enough to keep the holes fixed in co-moving coordinates for suitably chosen functions $a(\bar{t})$ and $\varphi(\bar{t})$.
- Since the motions of the holes are not known *a priori*, the functions $a(\bar{t})$ and $\varphi(\bar{t})$ must be chosen dynamically and adaptively as the system evolves.

Horizon Tracking Coordinates II

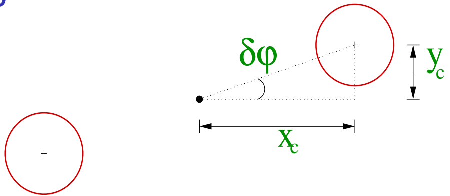

- Measure the co-moving centers of the holes: $x_c(t)$ and $y_c(t)$, or equivalently

$$Q^x(t) = \frac{x_c(t) - x_c(0)}{x_c(0)},$$

$$Q^y(t) = \frac{y_c(t)}{x_c(t)}.$$

Horizon Tracking Coordinates II

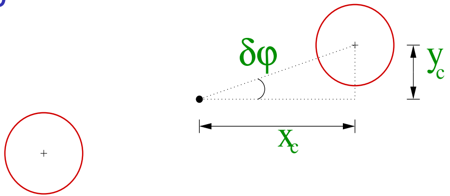

- Measure the co-moving centers of the holes: $x_c(t)$ and $y_c(t)$, or equivalently
$$Q^x(t) = \frac{x_c(t) - x_c(0)}{x_c(0)},$$
$$Q^y(t) = \frac{y_c(t)}{x_c(t)}.$$
- Choose the map parameters $a(t)$ and $\varphi(t)$ to keep $Q^x(t)$ and $Q^y(t)$ small.
- Changing the map parameters by the small amounts, δa and $\delta\varphi$, results in associated small changes in δQ^x and δQ^y:

$$\delta Q^x = -\delta a, \qquad \delta Q^y = -\delta\varphi.$$

Horizon Tracking Coordinates III

- Measure the quantities $Q^y(t)$, $dQ^y(t)/dt$, $d^2Q^y(t)/dt^2$, and set

$$\frac{d^3\varphi}{dt^3} = \lambda^3 Q^y + 3\lambda^2 \frac{dQ^y}{dt} + 3\lambda \frac{d^2Q^y}{dt^2} = -\frac{d^3Q^y}{dt^3}.$$

  The solutions to this "closed-loop" equation for Q^y have the form $Q^y(t) = (At^2 + Bt + C)e^{-\lambda t}$, so Q^y always decreases as $t \to \infty$.

Horizon Tracking Coordinates III

- Measure the quantities $Q^y(t)$, $dQ^y(t)/dt$, $d^2Q^y(t)/dt^2$, and set

$$\frac{d^3\varphi}{dt^3} = \lambda^3 Q^y + 3\lambda^2 \frac{dQ^y}{dt} + 3\lambda \frac{d^2Q^y}{dt^2} = -\frac{d^3Q^y}{dt^3}.$$

  The solutions to this "closed-loop" equation for Q^y have the form $Q^y(t) = (At^2 + Bt + C)e^{-\lambda t}$, so Q^y always decreases as $t \to \infty$.

- **This works!** This simple rotation plus expansion map allows us to evolve binary black holes to just before merger.

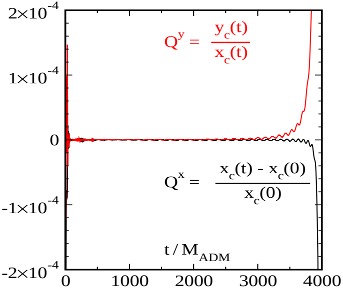

Horizon Tracking Coordinates III

- Measure the quantities $Q^y(t)$, $dQ^y(t)/dt$, $d^2Q^y(t)/dt^2$, and set

$$\frac{d^3\varphi}{dt^3} = \lambda^3 Q^y + 3\lambda^2 \frac{dQ^y}{dt} + 3\lambda \frac{d^2Q^y}{dt^2} = -\frac{d^3Q^y}{dt^3}.$$

The solutions to this "closed-loop" equation for Q^y have the form $Q^y(t) = (At^2 + Bt + C)e^{-\lambda t}$, so Q^y always decreases as $t \to \infty$.

- **This works!** This simple rotation plus expansion map allows us to evolve binary black holes to just before merger.
- More complicated maps that control the shapes of the horizons allow us to simulate the merger and ringdown as well.

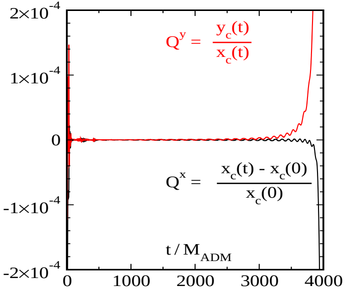

Caltech/Cornell Spectral Einstein Code (SpEC):

- Multi-domain pseudo-spectral method.

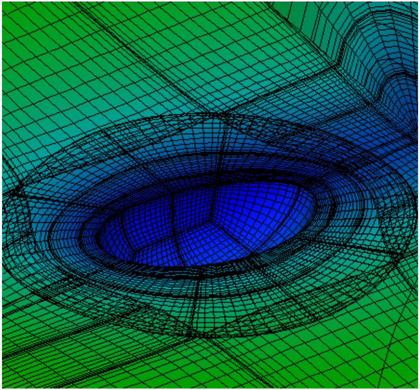

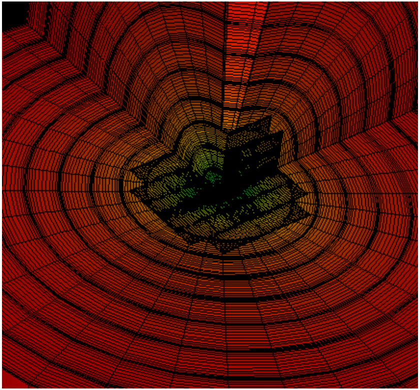

- Constraint damped "generalized harmonic" Einstein equations:

$$\Box g_{ab} = F_{ab}(g, \partial g).$$

- Constraint-preserving, physical and gauge boundary conditions.

Evolving Binary Black Hole Spacetimes

- We can now evolve BBH spacetimes with excellent accuracy and efficiency through many orbits plus merger plus ringdown.

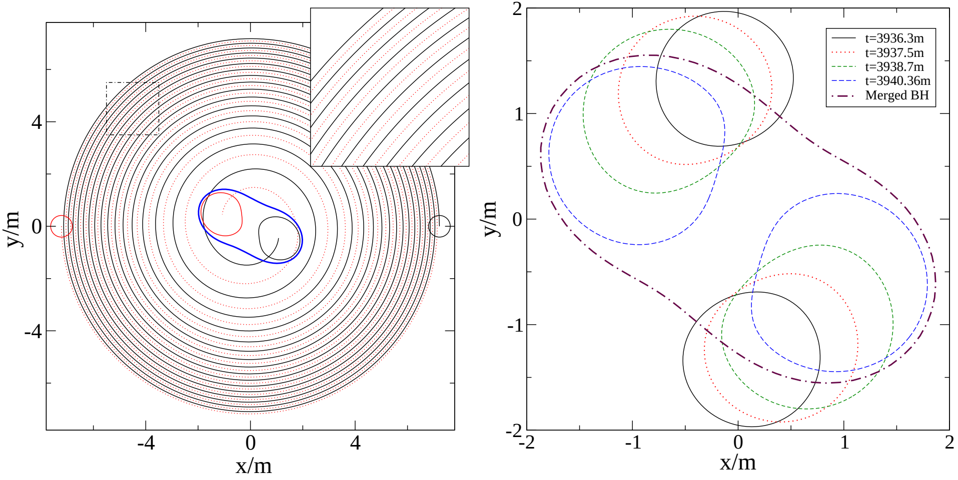

Head-on Merger Movie

Numerical Gravitational Waveforms

- We can now compute high precision gravitational waveforms for equal mass non-spinning BBH systems.

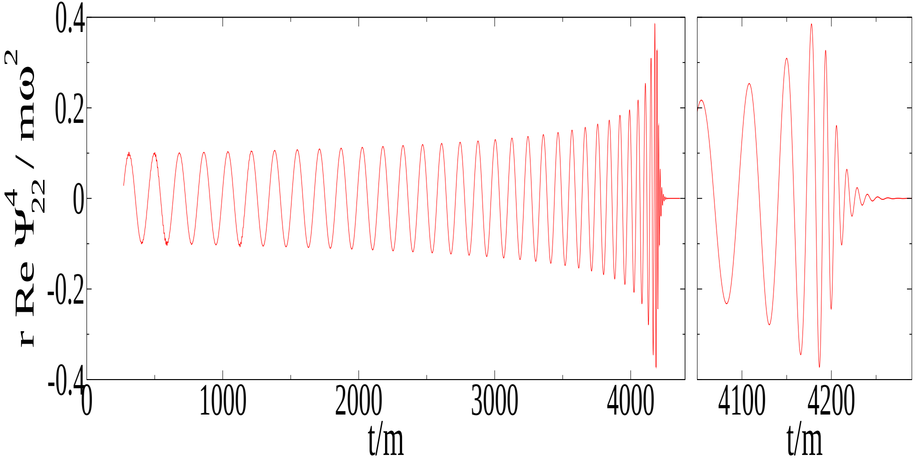

BBH Inspiral-Merger Movie

Post-Newtonian Gravitational Waveforms

- Until recently the only way to compute the gravitational waveforms predited by general relativity was through approximations.

Post-Newtonian Gravitational Waveforms

- Until recently the only way to compute the gravitational waveforms predited by general relativity was through approximations.
- The post-Newtonian approximation is an expansion of Einstein's equations appropriate for weak gravitational fields and slow moving sources.
- Post-Newtonian waveforms are very accurate for widely separated binary systems, but fail when the black holes get too close.

Post-Newtonian Gravitational Waveforms

- Until recently the only way to compute the gravitational waveforms predited by general relativity was through approximations.
- The post-Newtonian approximation is an expansion of Einstein's equations appropriate for weak gravitational fields and slow moving sources.
- Post-Newtonian waveforms are very accurate for widely separated binary systems, but fail when the black holes get too close.
- All current compact binary searches on LIGO use PN based waveform templates.

Post-Newtonian Gravitational Waveforms

- Until recently the only way to compute the gravitational waveforms predited by general relativity was through approximations.
- The post-Newtonian approximation is an expansion of Einstein's equations appropriate for weak gravitational fields and slow moving sources.
- Post-Newtonian waveforms are very accurate for widely separated binary systems, but fail when the black holes get too close.
- All current compact binary searches on LIGO use PN based waveform templates.
- **When do PN waveforms fail?**

Post-Newtonian Gravitational Waveforms

TaylorT1

1. Rewrite energy-balance equation

$$-\frac{dE_{\text{binary}}}{d\Omega}\frac{d\Omega}{dt}=\frac{dE_{\text{GW}}}{dt} \qquad \Rightarrow \qquad \frac{d\Omega}{dt}=-\frac{dE_{\text{GW}}/dt}{dE_{\text{binary}}/d\Omega}$$

2. Substitute Taylor series on right-hand side

$$\frac{d\Omega}{dt}=-\frac{\Omega^{10/3}\left(A_0+\ldots+A_n\Omega^{n/3}\right)}{\Omega^{-1/3}\left(B_0+\ldots+B_n\Omega^{n/3}\right)}$$

3. Numerically integrate once to find Ω
4. Numerically integrate once more to find Φ

Post-Newtonian Gravitational Waveforms

TaylorT4

1. Rewrite energy-balance equation

$$-\frac{dE_{\text{binary}}}{d\Omega}\frac{d\Omega}{dt} = \frac{dE_{\text{GW}}}{dt} \qquad \Rightarrow \qquad \frac{d\Omega}{dt} = -\frac{dE_{\text{GW}}/dt}{dE_{\text{binary}}/d\Omega}$$

2. Substitute Taylor series on right-hand side

$$\frac{d\Omega}{dt} = -\frac{\Omega^{10/3}\left(A_0 + \ldots + A_n\Omega^{n/3}\right)}{\Omega^{-1/3}\left(B_0 + \ldots + B_n\Omega^{n/3}\right)}$$

3. Re-expand right-hand side as a Taylor series, and truncate

$$\frac{d\Omega}{dt} = -\Omega^{11/3}\left(C_0 + \ldots + C_n\Omega^{n/3}\right)$$

4. Numerically integrate once to find Ω
5. Numerically integrate once more to find Φ

Post-Newtonian Gravitational Waveforms

TaylorT4

1. Rewrite energy-balance equation

$$-\frac{dE_{\text{binary}}}{d\Omega}\frac{d\Omega}{dt}=\frac{dE_{\text{GW}}}{dt}\qquad\Rightarrow\qquad\frac{d\Omega}{dt}=-\frac{dE_{\text{GW}}/dt}{dE_{\text{binary}}/d\Omega}$$

2. Substitute Taylor series on right-hand side

$$\frac{d\Omega}{dt}=-\frac{\Omega^{10/3}\left(A_0+\ldots+A_n\Omega^{n/3}\right)}{\Omega^{-1/3}\left(B_0+\ldots+B_n\Omega^{n/3}\right)}$$

3. Re-expand right-hand side as a Taylor series, and truncate

$$\frac{d\Omega}{dt}=-\Omega^{11/3}\left(C_0+\ldots+C_n\Omega^{n/3}\right)$$

4. Numerically integrate once to find Ω
5. Numerically integrate once more to find Φ

TaylorT2, ***TaylorT3***, ...

Comparing Various Order PN with NR Waveform

- Comparison of the numerical gravitational wave phase with predictions of various post-Newtonian orders.

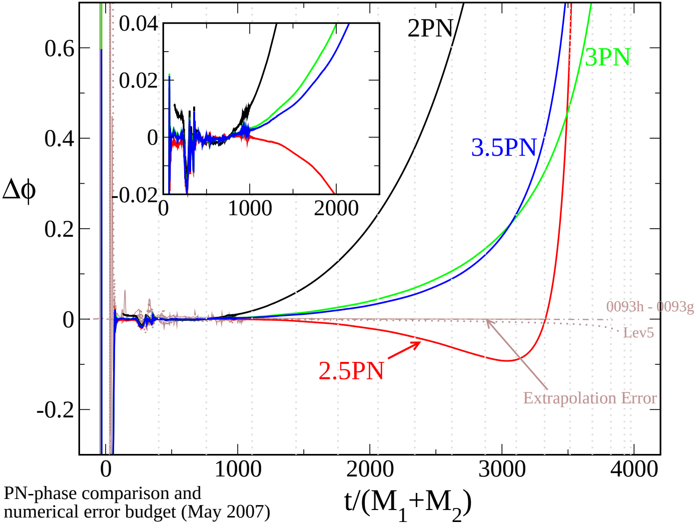

PN-phase comparison and numerical error budget (May 2007)

Comparing Various PN Methods

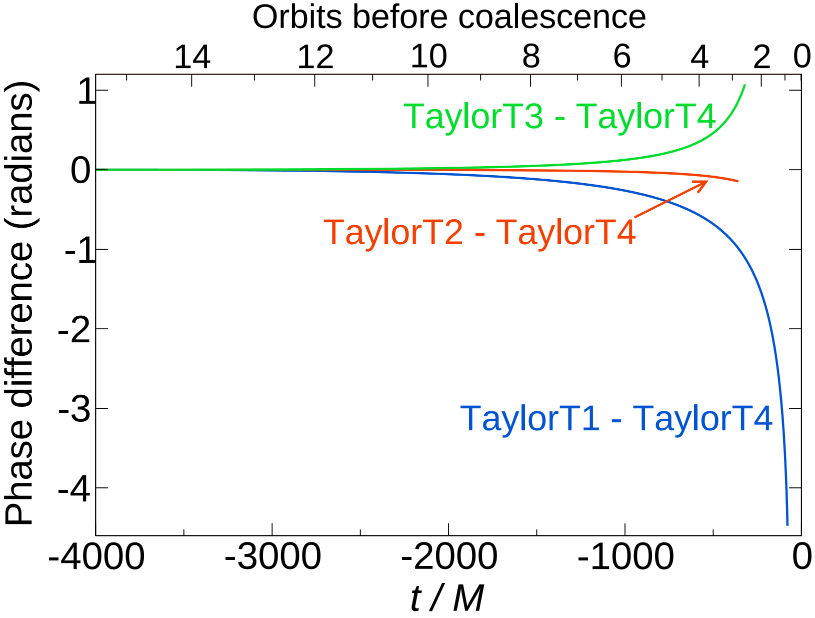

Comparing Various PN Methods with NR Waveform

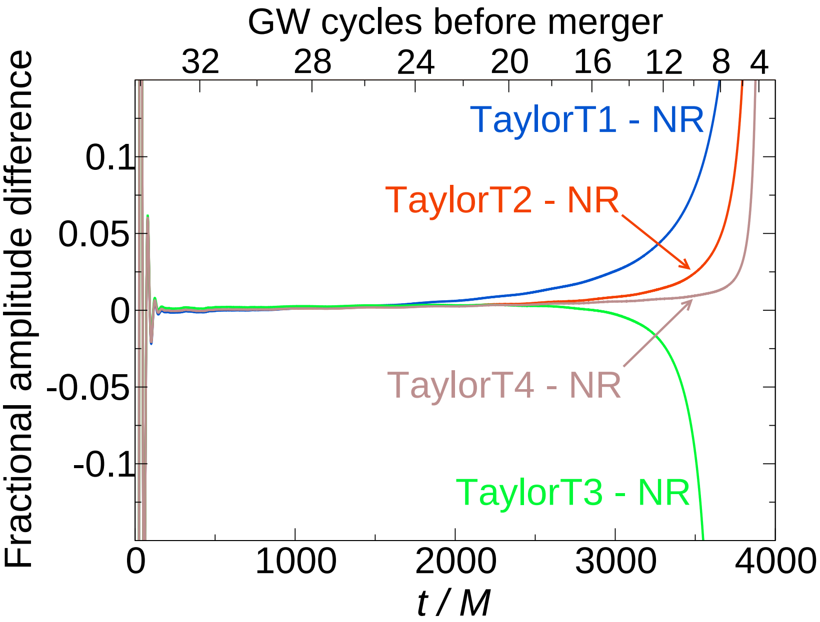

Comparing Various PN Methods with NR Waveform

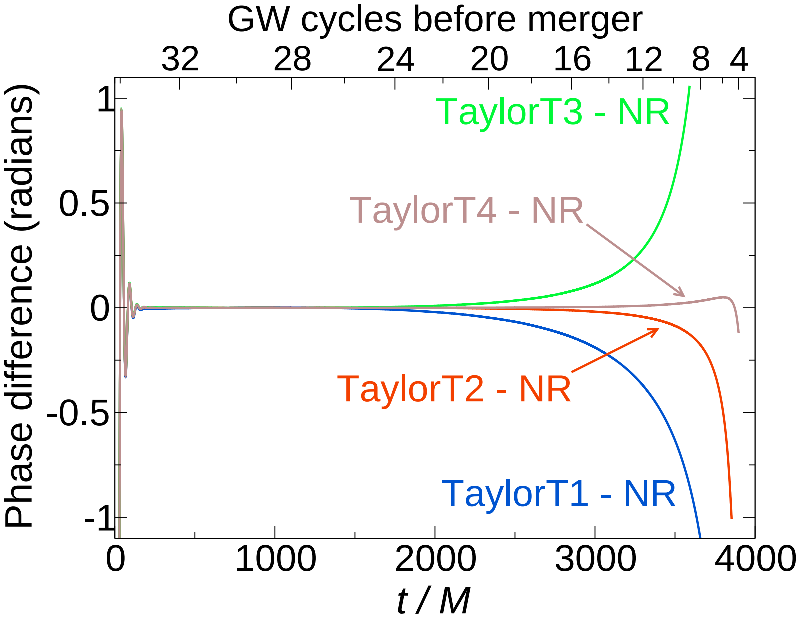

Summary

- Advances in understanding the Einstein equations provide new formulations suitable for numerical evolutions: hyperbolic formulations with constraint damping and well posed initial-boundary value problems.
- High accuracy multi-orbit binary black hole simulations are now routine (but not yet cheap).
- Numerical waveforms suitable for LIGO data analysis are starting to be generated.
- Interesting non-linear dynamics of binary black hole mergers are beginning to be investigated.